Computers and Concrete, *Vol. 26, No. 1* (*2020*) *95-106*
DOI: https://doi.org/10.12989/cac.2020.26.1.095

Effect of position of hexagonal opening in concrete encased steel castellated beams under flexural loading

G. Velrajkumar[1a] and M.P. Muthuraj[*2]

[1]*Department of Civil Engineering, SVS College of Engineering, Coimbatore, Tamil Nadu, 642 109, India*
[2]*Department of Civil Engineering, Coimbatore Institute of Technology, Coimbatore, Tamil Nadu,641 014, India*

(*Received February 3, 2020, Revised May 1, 2020, Accepted June 10, 2020*)

Abstract. Castellated beams fabricated from standard I-sections are being used for several structural applications such as commercial and industrial buildings, multistory buildings, warehouses and portal frames in view of numerous advantages. The advantages include enhanced moment of inertia, stiffness, flexural resistance, reduction in weight of structure, by passing the used plate girders, the passage of service through the web openings etc. In the present study, experimental and numerical investigations were carried out on concrete encased steel castellated beams with hexagonal openings under flexural loading. Various positions of openings such as along the neutral axis, above the neutral axis and below the neutral axis were considered for the study. From the experimental findings, it has been observed that the load-carrying capacity of the castellated beam with web opening above neutral axis is found to be higher compared to other configurations. Nonlinear finite element analysis was performed by using general purpose finite element software ABAQUS considering the material nonlinearities. Concrete damage plasticity model was employed to model the nonlinearity of concrete and elasto-plastic model for steel. It has been observed that FE model could able to capture the behaviour of concrete encased steel castellated beams and the predicted values are in good agreement with the corresponding experimental values.

Keywords: concrete; steel; castellated beam; flexural behavior; concrete damage model; finite element analysis

1. Introduction

Castellated beams are made from standard I-sections by making a cut along the web in a zigzag pattern and posteriorly reassembling the two parts by welding in a shifted configuration. Various advantages of castellated beams include (i) increased section height which results in enhanced moment of inertia, section modulus, stiffness, flexural resistance (ii) reduction in weight of structure (iii) optimum use of existing profiles (iv) by-passing the used plate girders and (v) the passage of service through the web openings.

The presence of opening in the web significantly affects the shear and buckling resistance of the beam, as a result, failure may occur in different or similar fashion than those observed in solid beams. It was reported in the literature that from various experimental findings on castellated beams, several failures were observed. The failures include (i) flexure mechanism formation (ii) overall beam lateral-torsional buckling (iii) vierendeel mechanism formation (iv) welded joint rupture in the web (v) web post-shear bucking (vi) web post-compression buckling; and (vii) tee compression buckling (viii) distortional buckling (Zainal and Izzuddin 2013, Kerdal and Nethercot 1984, Redwood and Demirdjian 1998, Juliet 2001, Zirakian and Showkati 2006, Ellobody 2011).

The castellated beams are commonly used as structural members in multistory buildings, commercial and industrial buildings, warehouses and portal frame.

Steel encased in reinforced concrete method is used to avoid the steel from buckling that can be used for beams, columns or coupling beams. There are two types of encased method, namely, fully encased and partially encased. In the fully encased method, the whole section is covered by the reinforced concrete so that the top and the bottom flanges are not in the outermost position. In this case, maximum strain developed in the steel is less than the one in the concrete. On the contrary, in partially encased method, only the web is covered by the reinforced concrete, therefore maximum strain will develop in steel flanges that make the application of the steel section can be more optimum.

Kerdal and Nethercot (1984) reviewed the failure modes of castellated beams and verified them against the experimental data available in the literature. Liu and Chung (2003) investigated the behavior of a castellated beam having different opening shapes and dimensions using finite element analysis and it was found that the castellated beam with octagonal openings exhibited better structural performance than that with hexagonal openings. Experimental and analytical investigations were carried out on distortional buckling of castellated beams by Tadeh and Hossein (2006). Experimental investigation on mechanism of C channel embedment section failure was carried by Liu *et al.* (2017). Experimental and numerical investigations were carried out by Salah and Gizejowski (2008a, 2008b) to study the stability behavior of slender section steel concrete

*Corresponding author, Assistant Professor
E-mail: muthuraj@cit.edu.in
[a]Assistant Professor

ISSN: 1598-8198 (Print), 1598-818X (Online)

composite beams with web openings. Ju *et al*. (2009) carried out experimental studies on composite beams using asymmetrical sections with web openings. The sections were filled with concrete on their side and top area, and the longitudinal shear resistance was obtained through the adhesion in the steel-concrete interface, as well as through the mechanical bracing of the concrete in the openings. Amir Hossein *et al*. (2011) proposed a model by using gene expression programming (GEP) to predict the load carrying capacity of castellated steel beams. To benchmark the GEP model a multiple least squares regression analysis is performed. Further, sensitivity analysis is performed to identify the contribution of related parameters affecting the load carrying capacity. It was mentioned that the model is effectively capable in predicting the failure load of the castellated beams. Gizejowski and Salah (2011) investigated the behavior of statically indeterminate single and multi-span composite beams (plain-webbed and castellated) using the FE analysis. Soltani *et al*. (2012) developed a numerical model using nonlinear finite element analysis to predict the failure load of castellated beams with hexagonal and octagonal openings. Both material and geometrical nonlinearities were considered in the finite element model. It was observed that web-posts in the castellated beams with octagonal openings was more susceptible to shear buckling than with hexagonal openings, for the existence of an intermediate plate in the web-post between two octagonal openings. Huo and D'Mello (2013) performed push-out tests to investigate the concrete-infill-only, tie-bar, ducting and web-welded stud shear connection in ultra-shallow floor beams. Braun *et al*. (2015) developed a composite slim-floor beam characterised by a concrete dowel placed between the flanges of a hot-rolled section with reinforcing bars passing through the openings and a concrete infill. Richard *et al*. (2017) performed numerical analysis of hexagonal castellated beam under monotonic loading to predict the failure load. It was found that the predicted values are in close agreement with that of experimental observations. Julia *et al*. (2019) developed explicit equations for the prediction of elastic local buckling critical stress of castellated beams subjected to pure bending, considering the interaction between flange and web. It was shown that this buckling mode is more relevant for castellated beams using high-strength steel. Moscoso *et al*. (2017) carried out numerical simulation of strengthening of steel concrete composite beam with pre-stressing tendon at steel web. It was found that the difference of numerical and experimental collapse values within 8%. Liu *et al*. (2020) performed numerical investigations on Web-post buckling of bolted castellated steel beam (BCSB) with octagonal web openings. From the studies, it was observed that web-posts in a BCSB with octagonal web openings exhibited as good structural performance as those in a traditional Welded Castellated Steel Beam. Dias *et al* (2015) carried out time dependent FEA of steel concrete composite beam with partial interaction. The beam and slab interface the Creep and shrinkage of concrete is caused due to time dependent deformation.

Ahmad *et al.* (2018) carried out the analytical and experimental investigation on the flexural behavior of partially encased composite beams. It was found that encased steel beam with circular opening having higher load carrying capacity. Yunitaidris and Togayozbakkaloglu (2014) carried out on flexural behavior of FRP -HSC steel composite beam. It was found that the double skin outer FRP and steel beam behavior similar to concrete encased steel I section with outer FRP. Afefy *et al.* (2012) carried out behavior of strengthened composite castellated beams pre-stressed with external bars: experimental study. It was found that web encased beam has greater performance. Ali *et al*. (2012) carried out strength and ductility of concrete encased composite beams. It was observed that ultimate load by predicted method is exceed the design value. Dabaon *et al.* (2003) carried out the experimental and theoretical study of curved rolled and castellated composite beams. It was observed that composite rolled castellated beam have higher performance than curved rolled composite beam. Jiang *et al.* (2016) carried out investigation on partially concrete encased composite beams under hogging moment. There is no slip bond failure between concrete and steel. Elakeya *et al.* (2016) studied on the structural behavior of concrete encased steel composite member. Satisfactory analytical and experimental result is obtained. Li *et al.* (2012) carried out the flexural behavior of GFRP-reinforced concrete encased steel composite beams. The stiffness and flexural strength of encased beam is higher. Mahmoud (2016) carried out finite element modeling of steel concrete beam considering double composite action. Measure the performance from load deflection curve. Chen and Cheng (2008) studied the flexural analysis and design methods for SRC beam sections with complete composite action. To compare the test results with predicted test by different methods. Leng and Song (2017) carried out flexural and shear performance of steel-concrete-steel sandwich slabs under concentrate loads. It was found that failure of slab occur suddenly. Samadhan *et al*. (2015) carried out an experimental and parametric study on steel beams with web openings. It was found that steel beam with circular web opening was effective. Hadi and Yuan (2017) carried out the experimental investigation of composite beams reinforced with GFRP I-beam and steel bars. It was found that position of I section move towards centre the strength was decrease. Weng *et al.* (2001) carried out the shear strength of concrete - encased composite structural members. It was found that shear capacity are predicted by method of super position. Vasdravellis and Uy (2014) carried out the shear strength and moment-shear interaction in steel-concrete composite beams. It was found that the depth of slab increases the shear strength also increases. Damage and stiffness research on steel shape steel fibre reinforced concrete composite beams was carried out by Xu *et al.* (2019). Liang *et al*. (2005) studied strength analysis of steel-concrete composite beams in combined bending and shear. Moment shear interaction equation was developed. Sener *et al.* (2016) performed the experimental and numerical investigation of the shear behavior of steel-plate composite (SC) beams without shear reinforcement. Shear strength and ductility results are satisfied with FEA result. He *et al.* (2012) carried out the shear behavior of partially encased composite I-

Table 1 mix proportion

Cement	Fine aggregate	Coarse aggregate	Water cement ratio
1	1.53	2.85	0.45

Table 2 Physical properties of material

Cement		Aggregate		
Physical property	Value	Property	Fine aggregate	Coarse aggregate
Fineness	6.00	Specific gravity	2.62	2.87
Specific surface, m^2/kg	255	Fineness modulus	2.78	6.12
Normal consistency (%)	32	Unit weight (kg/m^3)	1635	1590
Setting time (min) Initial Final	35 225			
Compressive strength (MPa) (28 days)	58			
Specific gravity	3.12			

girder with corrugated steel web: Numerical study. It was observed that shear strength of beam increase with thickness, height and compressive strength of concrete.

Concrete encased castellated beam provides higher strength and better performance compared to the encased steel beam. Same steel beam by converting into castellated beam, the depth of beam increased without adding any addition weight. So total weight of building/structure will be reduced and economical design will be achieved. Normal castellated beam has opening at neutral axis of beam.

From the available literature, it was observed that only limited investigations were reported on concrete encased steel beam with web opening at neutral axis. To the best of authors' knowledge, no studies were reported on the effect of various position of opening of castellated beam. The present research study mainly focused on the effect of opening position on the performance of the concrete encased castellated beam. From the study, it was found that the position of opening has pronounced effect on the strength of beam.

In the present study, experimental and numerical studies were carried out on castellated beams with hexagonal opening under flexural loading. Castellated beams were prefabricated by keeping the hexagonal openings along the neutral axis, above the neutral axis and below the neutral axis. Concrete damage plasticity model was employed to model the nonlinearity of concrete in compression and tension. General purpose finite element software, ABAQUS was used for finite element analysis. Concrete nonlinearity has been modelled by employing concrete damage model available in ABAQUS whereas steel nonlinearity is through elasto-plastic model.

2. Experimental investigations

The cement used was 53 grade Ordinary Portland Cement (OPC). The mix proportion was given in Table 1. The target compressive strength is M25. Physical properties of cement, fine aggregate and coarse aggregate are presented in Table 2. Average compressive strength (cube, 100×100×100 mm), split tensile strength (cylinder, 100×200 mm) and flexural strength (prism, 100×100×500 mm) of concrete at 28 days are obtained as 32, 3.2 and 4.15 MPa respectively.

The size of the beam is 150 mm×250 mm×2000 mm. Total five beams were cast and the geometry details are shown in Table 3.

The current investigation of concrete encased steel beam with different position of opening was studied and compared with numerical analysis. One reinforced concrete beam (CB), one concrete encased steel beam and three concrete encased steel beam with various position of opening such as at NA, above NA & below NA were studied experimentally. The beams were tested under two point loading. The cross sectional a detail of concrete beam is 150 mm× 250 mm with 2000 mm in length and steel and castellated beam are shown in Table 3.

2.1 Fabrication of castellated beams and wooden mould

Hot rolled steel beams were purchased from local market. Fabrication is required to convert the steel beam into castellated beam. Fabrication of castellated beam was carried out in workshop. First phase cutting of rolled beam along the web of the beam with zig zag pattern as shown in Fig. 6. Second rejoin of two halves and connected by arc

Table 3 Geometry details of beam

Details	CB	CESB	CESB H1	CESB H2	CESB H3
Reinforcement	Top 2 # 10mm Bottom 2# 12mm Stirrups 8 mm 200mm c/c	NA	NA	NA	NA
Breadth of flange (mm)	NA	65	65	65	65
Thickness of flange (mm)	NA	5	5	5	5
Height of web (mm)	NA	115	140	140	140
Thickness of web (mm)	NA	5	5	5	5
Shape of opening (mm)	NA	NA	hexagonal	hexagonal	hexagonal
Spacing of opening (mm)	NA	NA	50	50	50
Depth of opening (mm)	NA	NA	50	50	50
Position of opening	NA	NA	at Neutral axis	above Neutral axis	below Neutral axis

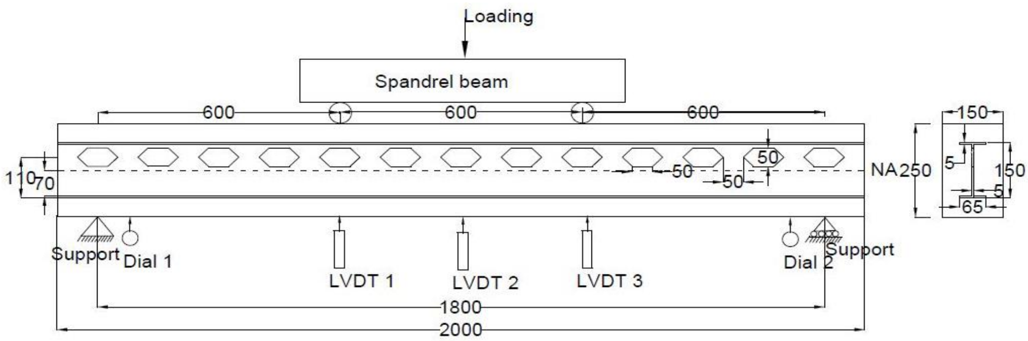

Fig. 1 Loading setup of concrete encased steel castellated beam opening above NA (CESB- H2)

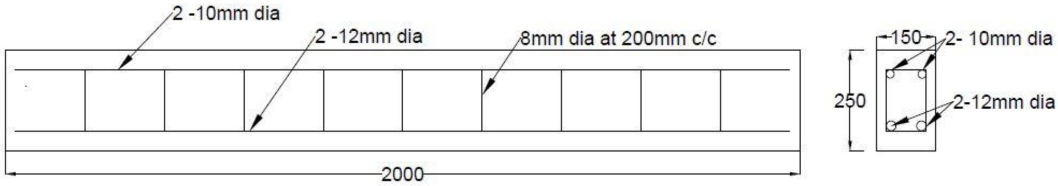

Fig. 2 Conventional beam (CB)

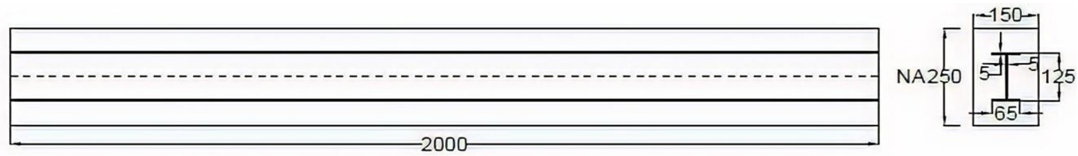

Fig. 3 Concrete encased steel beam (CESB)

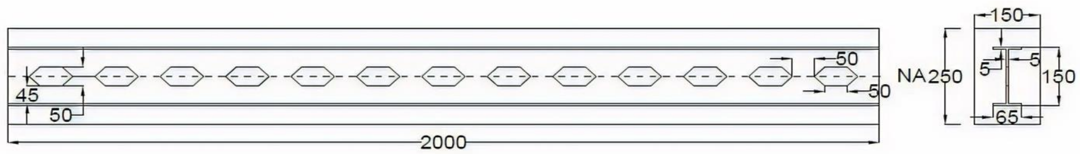

Fig. 4 Concrete encased steel castellated beam opening at NA (CESB- H1)

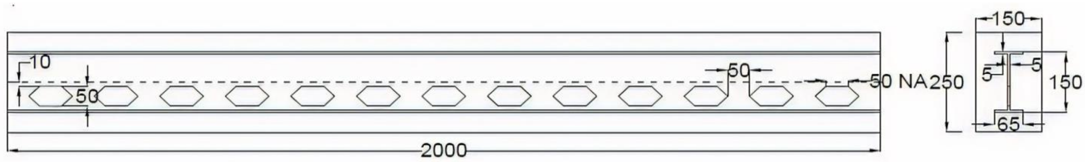

Fig. 5 Concrete encased steel castellated beam opening below NA (CESB- H3)

welding so that it will increase the overall depth of beam without adding additional weight. Due to the increasing of web depth, higher strength can be achieved and cost effective. For the long span structures, it reduces number of intermediate columns, result in economy foundation.

The plywood of 8 feet by 4 feet with 12 thick were purchased from market and fabricated to required shape of beam.

2.2 Casting of beams

The M25 grade concrete was designed as per Indian standard code. The steel beam and reinforcement were properly placed with clear cover. The concrete is prepared and poured into the mould and allowed for 28 days curing after demoulding. Simultaneously cubes, cylinder and prism were cast and slump was tested on fresh concrete.

2.3 Testing of beams

The loading frame of 500 kN was used for testing of beams. The two point load was applied gradually using hydraulic jack. The load cell was used to apply the load carefully. The three linearly variable differential transducer (LVDT) and two dial gauge are used to measure the deflection. The LVDTs are placed under loading point and mid span of beam and dial gauge was mounted at the supports.

The schematic diagrams are shown in Figs. 1 to 5.

Fabrication of typical castellated beams is shown in Fig. 6.

After 28 days of curing, all the beams were tested under

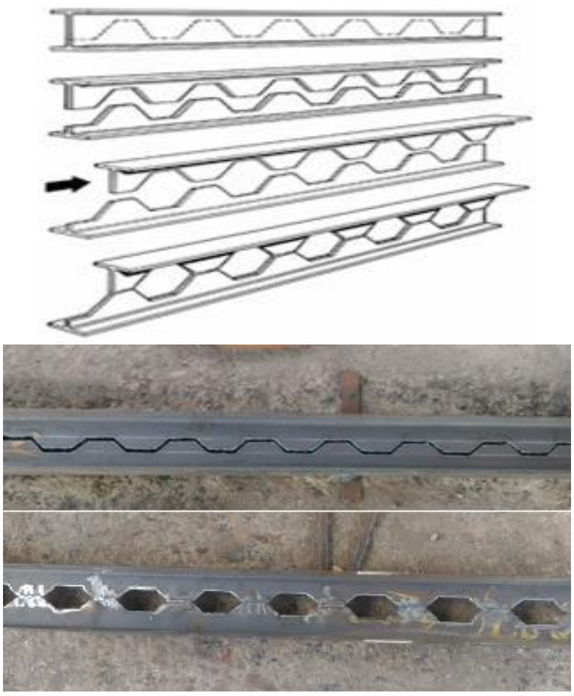

Fig. 6 Fabrication of castellated beams

Fig. 7 Typical test set up

four point bending as shown in Fig. 7. Deflections were measured by using LVDT.

Fig. 8 presents typical failure patterns of tested beams.

Load vs deflection obtained from the experiment is presented in Fig. 9 for all the cases. In general, it was observed that the performance of the concrete encased castellated beam is superior than the conventional RC beam. Further, it was also observed that the web opening and position of the opening plays a significant role on the load carrying capacity. From Fig. 9, it can be noted that the ultimate load for the case of control beam is 111 kN and the corresponding deflection is 16.845 mm. The ultimate load for the case of concrete encased steel castellated beam is (CESB) 132 kN and the corresponding deflection is 20.577 mm. The % increase of ultimate load is about 18.9% compared to control beam. From Fig. 9, it can be noted that (i) the ultimate load increases for all the cases of hexagonal openings and positions (CESB H1, CESB H2, CESB H3) (ii) maximum ultimate load is realized for CESB H2 where in the castellated beam with hexagonal opening is placed above the neutral axis. The load is 160 kN and the

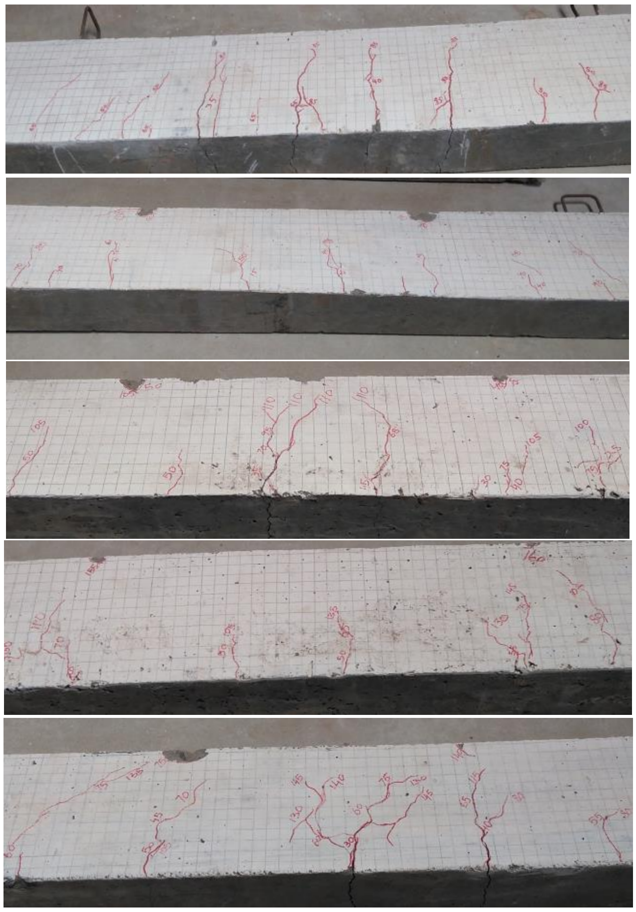

Fig. 8 Typical failure pattern of concrete castellated beams (CB, CESB, CESB- H1, CESB- H2 and CESB- H3)

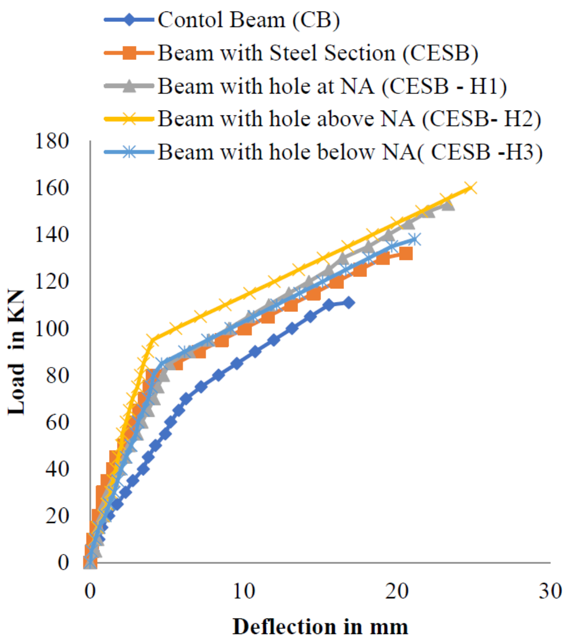

Fig. 9 Experimental load vs deflection

corresponding deflection is 24.794 mm. Compared to control beam, the capacity is increased to 44.14% without compromising the deflection. From Fig. 8, it can be seen that all the beams experienced flexural cracks and failed by crushing of concrete. The failure of CESB H2 is observed to be influenced by shear also.

2.4 Effect of position of hexagonal web opening

The first cracking load of control beam is 35 kN but concrete encased steel beam is 15 kN, which is lower than the control beam. Yield load and ultimate load of CESB is 80 kN and 132 kN respectively which are higher than the control beam. The initial cracking occurred for concrete steel castellated beam with opening at neutral axis (CESB -H1) is 30 kN which is higher than the encased beam. The yielding and ultimate loads are 85 kN and 153 kN, are higher than the control and encased steel beam. For the case of the concrete steel castellated beam with opening above neutral axis (CESB -H2), the first crack occurred at 20 kN and corresponding yielding and ultimate loads are 95 kN and 160 kN respectively, higher than all other cases. The first crack occurred in concrete steel castellated beam with opening below neutral axis (CESB -H3) is 30 kN and yielding and ultimate load are 85 kN and 138 kN respectively, higher than concrete encased beam but lower than concrete encased steel castellated beam opening above neutral axis.

2.5 Failure modes

The first crack of CB was observed at a load of 35 kN on left side under the loading point and gradually progressed towards top. Further, with the increase of load, multiple cracks were developed and final failure occurred due to crushing of concrete at a load of 111 kN.

For CESB, the first crack occurred at 15 kN near to underneath of loading point and the ultimate load is 132 kN. Beam failed after crushing of concrete.

In CESB-H1, the initial crack was observed at 30 kN in tension zone. The ultimate crushing of concrete occurred at 153 kN. The initial crack of CESB-H2 occurred at left side underneath of loading point at a load of 20 kN. The shear cracks were developed at the both ends of beam and ultimate crushing of concrete occurred at two loading points at a load of 160 kN.

The initial flexural crack in CESB-H3 occurred at a load 30 kN. As the load increases, the shear and flexural cracks were developed and ultimate crushing failure occurred at 138 kN. The flexural cracks were initially originated for the beams in the middle portion and shear cracks were observed near the supports. The failure of the beams is attributed to shear and flexural cracks.

3. Finite element analysis

The main objective of the finite element analysis is to predict the response of the castellated beams (Load vs deflection) and confirm the experimental findings. After the validation of FE modes, many parametric studies can be carried out without carrying the experiments. The validation part has been achieved in the present study. The optimum FE mesh has been arrived at after carrying out several mesh sensitivity studies.

There are two major failure mechanisms w.r.t simulation of concrete behavior. They are concrete cracking under tension and crushing under compression. But, concrete strength determined in simple states of stress either through simple tension and compression tests significantly differs from that established in complex states of stress. To simulate the behavior of concrete in complex state, the Concrete Damaged Plasticity (CDP) model can be effective choice. The CDPM is effective for monotonic, cyclic, and dynamic loading under low confining pressures. Isotropic tensile plasticity and isotropic compressive plasticity are used to represent the inelastic behavior of concrete. To predict the realistic behavior of reinforced concrete beam, it is essential to consider several aspects in the modeling.

It is important to note that the modeling of (i) RC beam (ii) concrete encased steel beam (iii) concrete encased steel beam with hexagonal opening requires special attention to predict the realistic behavior. Several aspects are to be considered in the modeling that includes (i) compression and tensile behavior of concrete (ii) fracture energy (iii) damage parameters (iv) constitutive relationship of reinforcing material. In the present study, nonlinear finite element analysis has been carried out to predict the behavior of (i) RC beam (ii) concrete encased steel beam (iii) concrete encased steel beam with hexagonal opening. ABAQUS, a general purpose finite element software has been employed to model and analyze the beam. To model the nonlinearity of concrete, Concrete damage plasticity model was employed. The concrete damage plasticity model is based on a coupled damage plasticity theory and the multi-axial behavior of concrete in damaged plasticity model governs by a yield surface which is proposed by Lubliner *et al*. (1989) and was later modified by Lee and Fenves (1998). Tensile cracking and compressive crushing of concrete are two assumed main failure mechanisms in this model. Furthermore, the degradation of material for both tension and compression behaviors have been considered in this model. The Concrete damage plasticity (CDP) model is the modified version of Druker-Prager strength hypothesis where in the failure cross-section in the deviatoric plane can be of any shape, which is determined by the parameter K_c (Lubliner *et al*. 1989). K_c is the ratio of distances between hydrostatic axis and compression and tension meridians, respectively, in the deviatoric cross-section. The major input for CDP model include K_c, σ_{b0}/σ_{c0} (the ratio of compressive strength in bi-axial state to that in uni-axial state), dilation angle (ψ), eccentricity (ε) and viscosity (μ), along with the stress-strain behaviors in compression and tension and variation of damage with inelastic strain (in compression) and with cracking strain (in tension). Dilation angle, ψ, is the angle of inclination of the failure surface towards the hydrostatic axis, measured in the meridional plane. Physically, it can be understood as the angle of internal friction of concrete. Eccentricity Parameter can be calculated as the ratio of tensile strength to compressive strength (Jankowiak 2005). The viscosity parameter slightly helps in reduction in the step size, in order to regularize the constitutive equations. For non-viscoelastic materials, the value is recommended to be 0 (Kmiecik and Kaminski 2011).

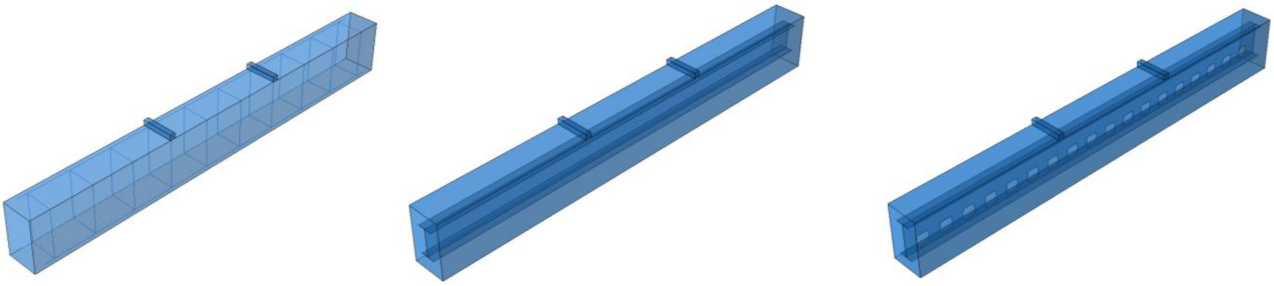

(a) Conventional beam (b) Concrete encased steel beam (c) Concrete encased steel beam with opening

Fig. 10 Typical geometry

Table 4 Material properties (Elastic)

Material	Properties	Value
Concrete	Grade of concrete	M25
	Young's modulus (MPa)	28722.8
	Poisons ratio	0.2
	Compressive strength (MPa)	32
Reinforcement	Grade of Steel	Fe550
	Young's modulus (MPa)	2.01×10^5
	Poisons ratio	0.3
	Yield stress (MPa)	587
Structural Steel	Young's modulus (MPa)	2.01×10^5
	Poisons ratio	0.3
	Yield stress (MPa)	265
	Ultimate stress (MPa)	435
Bearing Plate	Young's modulus (MPa)	2.01×10^5
	Poisons ratio	0.3

Table 5 Compressive behavior of concrete

Inelastic strain	Yield Stress (MPa)	Damage in Compression (d_c)
0	0	0
0	12.25	0
0.000131	21.47194	0.008034
0.000383	27.66423	0.023495
0.000761	30.72992	0.046618
0.001744	31.14516	0.106875
0.00229	29.99439	0.140332
0.003412	26.96133	0.209041
0.003974	25.41181	0.243476
0.005088	22.55983	0.311741
0.005638	21.28992	0.34549
0.006728	19.05919	0.412232
0.007802	17.19287	0.478081
0.008865	15.62614	0.543196
0.012002	12.19726	0.735423
0.01252	11.76031	0.767132
0.014065	10.61292	0.861856

Table 6 Tensile behavior of steel

Yield Stress (MPa)	Tensile Strain
448	0
475	0.0001
504	0.0003
532	0.001
587	0.002
587	0.003
594	0.005
587	0.01
540	0.03
500	0.06

3.1 Modelling aspects

The concrete beam is modeled with the brick elements to achieve the uniform stress distribution. C3D8R (Cube Three-Dimensional eight node Reduced integration) elements with three degrees of freedom are used to the concrete part of beam where in elements use linear interpolation in each direction and often called linear elements of first order elements. A two noded truss element is used for modeling of reinforcing steel rebars (T3D2). Castellated steel I-beams are modeled as three-dimensional shell element (S4R) A 4-node quadrilateral shell element with each node having three translational and three rotational degrees of freedom. This element has finite film strain and linear reduced integration. S4R can be used for both thin shell as well as thick shell models because of its good adaptability. The S4R element uses a reduced integration rule with one integration point that makes this element computationally less expensive than S4. Fig. 10 shows the typical geometry models.

The constitutive post-cracking relationships for concrete, plastic effects of the reinforcements and structural steel were considered in the analysis to simulate the possible failure phenomenon of the concrete beam through effective load transfer mechanism at the nodes beyond the post yielding of concrete. The concrete part was defined as a three-dimensional "Deformable" body, meaning it is a part that can be of arbitrary shape and that can deform under mechanical, thermal, or electrical loading. The concrete in all analyses performed in this study was modelled using continuum elements. These elements are advantageous for modelling three-dimensional nonlinear problems involving plasticity and large deflections.

In order to predict accurate results from the FE model, all the elements in the model were discretized to same mesh size to ensure that each of two different materials shares the same node. Compatibility of all the connecting elements have been ensured.

3.2 Material properties

The Concrete is a quasi brittle material and has different

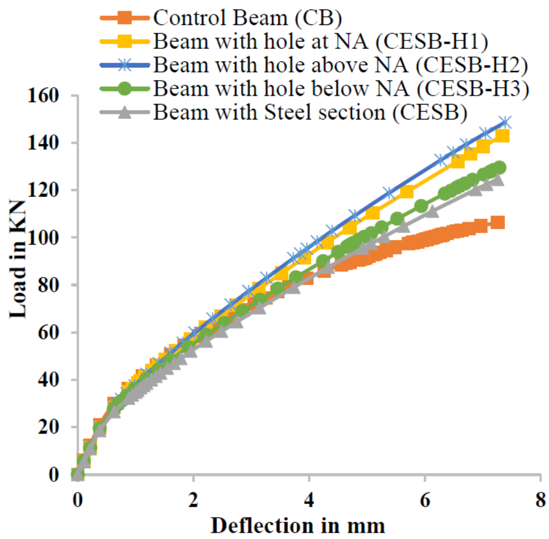

Fig. 11 Numerical load vs deflection

Table 7 Ultimate load and deflection

Specimen	Ultimate load (kN)		Ultimate Deflection(mm)	
	FEA	Experimental	FEA	Experimental
CB	106.4	111	7.259	16.845
CESB	124.5	132	7.257	20.577
CESB H1	142.9	153	7.344	23.347
CESB H2	148.6	160	7.387	24.794
CESB H3	129.4	138	7.287	21.153

behavior in tension and compression. The cracking and crushing stresses are derived from compressive and tensile strength of concrete. The elastic perfectly plastic material properties are assumed for reinforcement in modeling. The material properties are shown in Tables 4, 5 and 6.

Simply supported boundary conditions such as hinge and roller are simulated for all the beams. Displacement based loading was applied to the beam with a constant displacement of 8 mm for all the beams. For a relative comparison of all the cases a constant input displacement of 8mm was chosen for the analysis as a reference value to check the load carrying capacity of castellated beams. Nonlinear finite element analysis was carried out by using finite element tool ABAQUS CAE 6.14. Load-deflection values of beams were obtained from finite element software ABAQUS. Deflection for every increment of load was captured. The deflections were increased linearly up to elastic region followed by a nonlinear trend. Concrete encased steel beam (CESB) has less deflection compared to control beam (CB) and exhibited less stress in bottom flange and web of CESB. Stress concentration is high in the opening of CESB H1 & CESB H2. The load-carrying capacity of steel-concrete composite beam is high compared to the conventional beam (RC beam). The load-carrying capacity of concrete-encased steel castellated beam with the opening above neutral axis is high. The load vs deflection of beams predicted by using ABAQUS 6.14 is shown in Fig. 11. From Fig. 11, it can be inferred that after first cracking,

the stiffness of the numerical load-deflection curves is again higher than that of the experimental beams. The reason could be the (i) micro cracks/pores and (ii) slip between the steel and concrete have not been modeled. The load carrying capacity for CESB-H2 is 28.3%, 16.2%, 12.9%, 3.8% more than the control beam, CESB, CESB-H3 and CESB-H1.

From Fig. 12(a), it can be observed that for a beam with opening below neutral axis the crack initiation and propagation is rapid compared to other cases. This is because of the fact that the concrete being weak in tension cracks at faster rate compared to opening above neutral axis which is in compression.

From the Fig. 12, it can be observed that the steel I section when the hole is above NA did not yield at its ultimate load carrying capacity whereas the section had yielded extensively when the hole is below NA. Concrete Damage plasticity model adopted in this study was able to capture the cracking characteristics of concrete and steel accurately. Table 7 compares the predicted and the experimental ultimate load and deflection for all the cases.

From Table 7, it can be noted that the predicted ultimate loads are in very good agreement with the corresponding experimental observations. The maximum percentage difference between the predicted and the experimental value is less than 10%, The deflection values cannot be compared. Because, in the analysis, the maximum deflection is limited to 8mm. However, it can be noted that the developed FE model could be able to predict the desired deflection. It can be inferred that the constitutive models employed for concrete and steel are able to capture the behavior of concrete beams reinforced with either rebars or structural steel.

Fig. 13 represents the typical contour plots of (i) cracking of concrete and (ii) damage of concrete in tension.

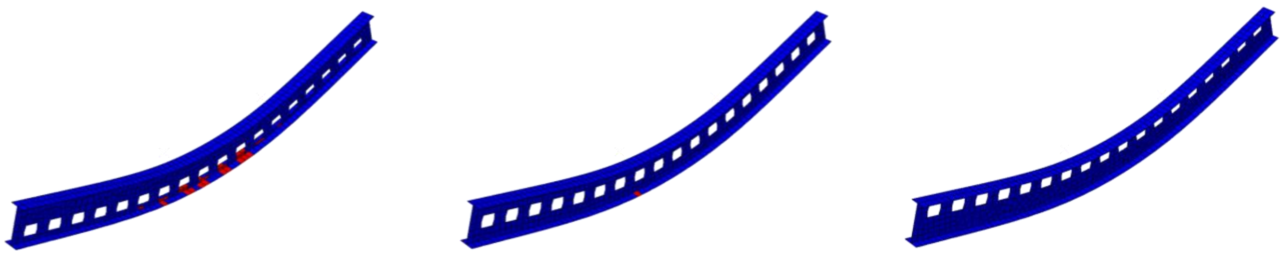

(a) Opening below NA (b) Opening along NA (c) Opening above NA

Fig. 12 Yielding of encased steel section

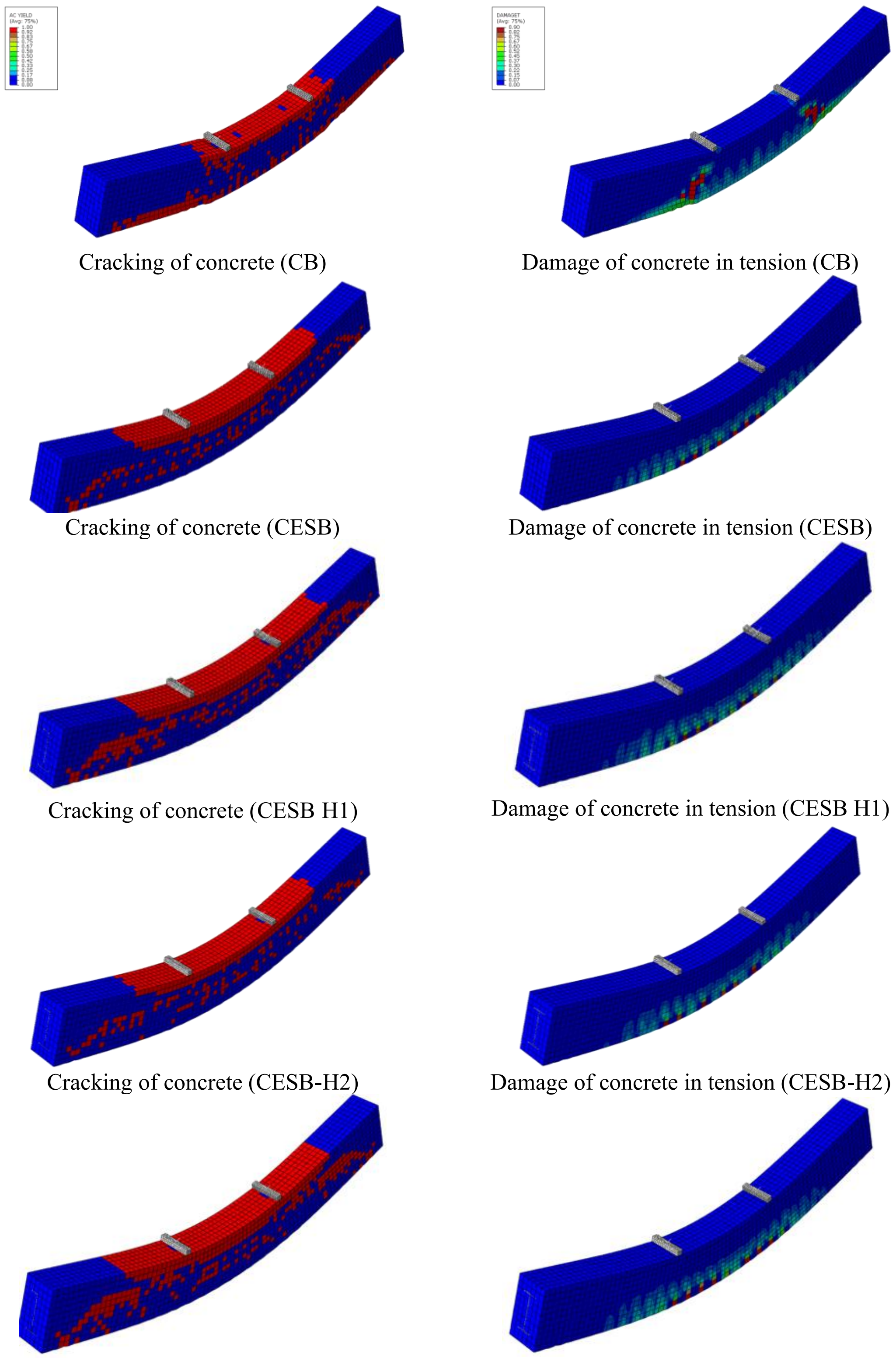

Cracking of concrete (CB) Damage of concrete in tension (CB)

Cracking of concrete (CESB) Damage of concrete in tension (CESB)

Cracking of concrete (CESB H1) Damage of concrete in tension (CESB H1)

Cracking of concrete (CESB-H2) Damage of concrete in tension (CESB-H2)

Cracking of concrete (CESB-H3) Damage of concrete in tension (CESB-H3)

Fig. 13 Typical contours for cracking of concrete and damage off concrete

It was observed that the concrete cracked extensively for the case of control beam compared to other cases.

3.3 Modelling simulation

The main aim of numerical investigation to validate the experimental observations and to carryout parametric studies. The material properties and geometry of beam are same as used for experimental studies. The same experimental conditions were applied to measure the numerical behavior of encased beam such as failure pattern, deflection of beam and ultimate load carrying capacity. The

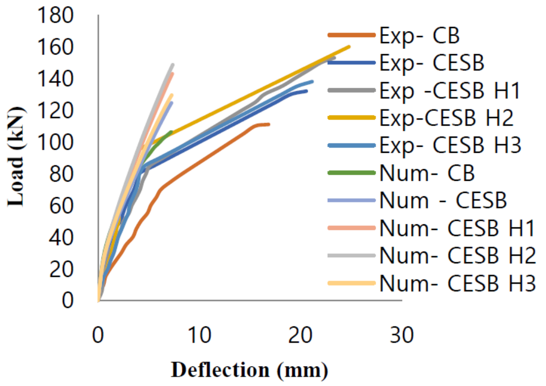

Fig. 14 Comparison of experimental and numerical values

comparison of experimental and numerical load vs deflection graph is shown in Fig. 14. The experimental and finite element behavior of concrete encased beams is coinciding upto the initial elastic region. Up to a load of 100 kN, the numerical behavior of stiffer. Numerical simulation is carried out by limiting the deflection up to 8mm. The predicted maximum load and the corresponding experimental load is fairly in good agreement with each other. The maximum difference is found to be less than 10%.

3.4 Failure modes from numerical analysis

The failure modes of numerical analysis are very closer to the experimental behavior such as ultimate load and failure pattern. The max shears cracks of CB obtained from numerical simulation are closer to experimental shear crack. The numerical cracking and crushing failure of CESB beam is similar to experimental observations. The stress in steel of CESB is within the safe permissible limit. All the beams are fails by crushing of concrete and cracking due to tension stress on concrete. From Fig. 12, it can be seen that max stress occurred for the castellated beam with hexagonal opening at NA compared to opening below neutral axis. The castellated beam with opening above NA experienced very low yielding stress occurred compared to opening below NA. The von mises stress of CB is about 544.6 MPa which is higher than the CESB i.e., 407.5 MPa. The von mises stress obtained for CESB-H2 is 436.1 MPa which is higher than the CESB-H2 which is about 404 MPa and lesser than the CESB-H1 whose value is 442.3 MPa

From Figs. 12 and 13, it has been observed that the maximum values are within the allowable values i.e. developed yield strength of structural steel is found to be less than the permissible value. Similarly the developed strain in concrete is less than the permissible value.

4. Conclusions

Experimental and numerical investigations were carried out on concrete encased steel castellated beams with hexagonal openings under flexural loading. For the investigation, various positions of openings such as along the neutral axis, above the neutral axis and below the neutral axis were considered. Maximum care has been taken to fabricate the steel sections such that alignment of the opening and position of the section maintained as planned. Experiments were carried out on castellated beams and load vs deflection was recorded for all the cases. From the experimental findings, it has been observed that the load-carrying capacity of the castellated beam with web opening above neutral axis is found to be higher compared to other configurations. Nonlinear finite element analysis was performed by using general purpose finite element software ABAQUS considering the material nonlinearities. Finite element model was created by considering the appropriate material model/constitutive relationship for concrete, reinforcement and structural steel and by employing appropriate constraint conditions as close to experimental conditions. Concrete damage plasticity model was employed to model the nonlinearity of concrete and elasto-plastic model for steel. It has been observed that FE model could able to capture the behaviour of concrete encased steel castellated beams and the predicted values are in good agreement with the corresponding experimental values. The ultimate load carrying capacity increases due to composite action. Encased castellated beam has more strength compared to all other specimens. The load-carrying capacity of the castellated beam influenced by the web opening and location of the opening. For the case of opening in compression zone, the strength of the beam is high. The maximum percentage difference between the predicted ultimate load and the corresponding experimental load is less than 10%. The developed FE model is found to be reliable and could capture the nonlinear behavior of the concrete encased steel castellated beams with hexagonal openings under flexural loading.

References

ABAQUS (2004), User Manual, Version 6.4, ABAQUS Inc., Pawtucket, Rhode, Island.

Abidin, A.Z. and Izzuddin, B.A. (2013), "Meshless local buckling analysis of steel beams with irregular web openings", *Eng. Struct.*, **50**, 197-206. https://doi.org/10.1016/j.engstruct.2012.10.006.

Adhikary, B.B., Mutsuyoshi, H. and Sano, M. (2000), "Shear strengthening of reinforced concrete beams using steel plates bonded on beam web: experiments and analysis", *Constr. Build. Mater.*, **14**(5), 237-244. https://doi.org/10.1016/S0950-0618(00)00023-4.

Afefy, H.M.E.D., Atta, A.M. and Taher, S.E.D.F. (2012), "Behavior of strengthened composite castellated beams pre-stressed with external bars: Experimental study", *Arab. J. Sci. Eng.*, **37**(6), 1521-1534. https://doi.org/10.1007/s13369-012-0278-2.

Ahmad, S., Masri, A. and Abou Saleh, Z. (2018), "Analytical and experimental investigation on the flexural behavior of partially encased composite beams", *Alex. Eng. J.*, **57**(3), 1693-1712. https://doi.org/10.1016/j.aej.2017.03.035.

Ali, A.A., Sadik, S.N. and Abdul-Sahib, W.S. (2012), "Strength and ductility of concrete encased composite beams", *Eng. Technol. J.*, **30**(15), 2701-2714.

Baskar, K., Shanmugam, N.E. and Thevendran, V. (2002), "Finite-element analysis of steel-concrete composite plate girder", *J. Struct. Eng.*, **128**(9), 1158-1168. https://doi.org/10.1061/(ASCE)0733-9445.

Chen, C.C. and Cheng, C.L. (2008), "Flexural analysis and design methods for SRC beam sections with complete composite action", *J. Chin. Inst. Eng*., **31**, 215-229. https://doi.org/10.1080/02533839.2008. 9671375.

Chen, C.C., Li, J.M. and Weng, C.C. (2005), "Experimental behaviour and strength of concrete-encased composite beam-columns with T-shaped steel section under cyclic loading", *J. Constr. Steel Res*., **61**(7), 863-88. https://doi.org/10.1016/j.jcsr.2005.01.002.

Chen, E.Y. and Schnobrich, W.C. (1981). "Material modeling of plain concrete", *Adv. Mech. Reinf. Concrete*, IABSE Colloquium, Delft, 33-51.

Chen, F.W. (1982), *Plasticity in Reinforced Concrete*, McGraw-Hill, New York.

Chen, S. and Gu, P. (2005), "Load carrying capacity of composite beams prestressed with external tendons under positive moment", *J. Constr. Steel Res*., **61**(4), 515-530. https://doi.org/10.1016/j.jcsr.2004.09.004.

Dabaon, M., El-Naggar, M.I. and Yossef, N.M. (2003), "Experimental and theoretical study of curved rolled and castellated composite beams", *Alex. Eng. J*., **42**(2), 219-230.

de Oliveira, J.P., Cardoso, D.C.T. and Sotelino, E.D. (2019), "Elastic flexural local buckling of Litzka Castellated beam: Explicit equation anf FE parametric study", *Eng. Struct*., **186**(1), 436-445. https://doi.org/10.1016/j.engstruct.2019.02.034.

De Sutter, S., Verbruggen, S. and Tysmans, T. (2016), "Shear behaviour of hybrid composite-concrete beams: Experimental failure and strain analysis", *Compos. Struct*., **152**(15), 607-616. https://doi.org/10.1016/j.compstruct.2016.05.075.

Dias, M.M., Tamayo, J.L., Morsch, I.B. and Awruch, A.M. (2015), "Time dependent finite element analysis of steel-concrete composite beams considering partial interaction", *Comput. Concrete*, **15**(4), 687-707. http://dx.doi.org/10.12989/cac.2015.15.4.687.

Durifa, S. and Bouchaira, A. (2012), "Behavior of cellular beams with sinusoidal openings", *Procedia Eng*., **40**, 108-113. https://doi.org/10.1016/j.proeng.2012.07.064.

Elakeya, U., Bhuvanesh, A. and Gajalakshmi, P. (2016), "Study on the structural behavior of concrete encased steel composite members", *Int. J. Earth Sci. Eng*., **9**(3), 323-329.

Ellobody, E. (2011), "Interaction of buckling modes in castellated steel beams", *J. Constr. Steel Res.*, **67**(5), 814-825. https://doi.org/10.1016/j.jcsr.2010.12.012.

Frans, R., Parung, H., Sandy, D. and Tonapa, S (2017), "Numerical modeling of hexagonal castellated beam under monotonic loading", *Procedia Eng.*, **171**, 781-788. https://doi.org/10.1016 /j.proeng. 2017.01.449.

Gandomi, A.H., Tabatabaei, S.M., Moradian, M.H., Radfar, A. and Alavi, A.H. (2011), "A new prediction model for the load capacity of castellated steel beams", *J. Constr. Steel Res*., **67**(7), 1096-1105. https://doi.org/10.1016/j.jcsr.2011.01.014.

Gizejowski, M.A. and Salah, W. (2011), "Numerical modeling of composite castellated beams", *Proceeding Local Seminar of the Polish Chapter of IASS*, Warsaw.

Gu, X., Chen, T., Li, H., Zhang, W. and Wang, H. (2012), "behavior of steel-concrete composite cantilever box beams under negative moment", *J. Constr. Steel Res*., **12**, 509-521. https://doi.org/10.1007/s13296-012-4005-3.

Hadi, M.N. and Yuan, J.S. (2017), "Experimental investigation of composite beams reinforced with GFRP I-beam and steel bars", *Constr. Build. Mater*., **144**, 462-474. https://doi.org/10.1016/j.conbuildmat.2017.03.217.

He, J., Liu, Y., Chen, A. and Yoda, T. (2012), "Shear behavior of partially encased composite I-girder with corrugated steel web: Experimental study", *J. Constr. Steel Res*., **77**, 193-209. https://doi.org/10.1016/j.jcsr.2012.05.005.

He, J., Liu, Y., Lin, Z., Chen, A. and Yoda, T. (2012), "Shear behavior of partially encased composite I-girder with corrugated steel web: Numerical study", *J. Constr. Steel Res.*, **79**, 166-182. https://doi.org/10.1016/j.jcsr.2012.07.018

Hsu, H.L. and Wang, C.L. (2000), "Flexural torsional behaviour of steel reinforced concrete members subjected to repeated loading", *Earthq. Eng. Struct. Dyn*., **29**(5), 667-682. https://doi.org/10.1002/(SICI)1096-9845(200005)29:5<667::AID-EQE930>3.0.CO;2-Y.

Huo, B.Y. and D'Mello, C.A. (2013), "Push out test and analytical study of shear transfer mechanisms in composite shallow cellular floor beams", *J. Constr. Steel Res.*, **88**, 191-205. https://doi.org/10.1016/j.jcsr. 2013. 05. 007.

Ibrahim, S.A., El-Dakhakhni, W.W. and Elgaaly, M. (2006), "Behavior of bridge girders with corrugated webs under monotonic and cyclic loading", *Eng. Struct*., **28**(14), 1941-1955. https://doi.org/10.1016/j.engstruct.2006.03.026.

Idris, Y. and Ozbakkaloglu, T. (2014), "Flexural behavior of FRP-HSC-steel composite beams", *Thin Wall. Struct*., **80**, 207-216. https://doi.org/10.1016/j.tws.2014.03.011.

Jankowiak, T. and Lodygowski, T. (2005), "Identification of parameters of concrete damage plasticity constitutive model", *Found. Civil Environ. Eng*., **6**(1), 53-69.

Jiang, Y., Hu, X., Hong, W., Gu, M. and Sun, W. (2016), "Investigation on partially concrete encased composite beams under hogging moment", *Adv. Struct. Eng*., **20**(3), 461-470. https://doi.org/10.1177/1369433216654148.

Ju, Y.K., Chun, S.C. and Kim, S.D. (2009), "Flexural test of a composite beam using asymmetric steel section with web openings", *J. Struct. Eng*., **135**(4), 448-458. https://doi.org/10.1061/(ASCE)0733-9445(2009)135:4 (448).

Kerdal, D. and Nethercot, DA. (1984), "Failure modes for castellated beams", *J. Constr. Steel Res.*, **4**(4), 295-315. https://doi.org/10.1016/0143-974X(84)90004-X.

Kmiecik, P. and Kamiński, M. (2011), "Modelling of reinforced concrete structures and composite structures with concrete strength degradation taken into consideration", *Arch. Civil Mech. Eng*., **11**, 623-636. https://doi.org/10.1016/S1644-9665(12)60105-8.

Lawson, M., Beguin, P., Obiala, R. and Braun, M. (2015), "Slim floor construction using hollow-core and composite decking systems", *Steel Constr*., **8**(2), 85-89. https://doi.org/10.1002/stco.201510018.

Lee, J. and Fenves, G.L. (1994), "Numerical implementation of plastic-damage model for concrete under cyclic loading: application to concrete dam", Rep. No. UCB/SEMM-94/03, Department of Civil Engineering, University of California, Berkeley, California.

Lee, J. and Fenves, G.L. (1998), "Plastic-damage model for cyclic loading of concrete structures", *J. Eng. Mech.*, **124**(8), 892-900. https://doi.org/10.1061/(ASCE)0733-9399(1998)124:8(892).

Lee, T.K. and Pan, A.D. (2001), "Analysis of composite beam-columns under lateral cyclic loading", *J. Struct. Eng*., **127**(2), 186-193. https://doi.org/10.1061/(ASCE)0733-9445(2001)127:2(186).

Leng, Y.B. and Song, X.B. (2017), "Flexural and shear performance of steel-concrete-steel sandwich slabs under concentrate loads", *J. Constr. Steel Res.*, **134**, 38-52. https://doi.org/10.1016/j.jcsr.2017.03.009

Li, L.Z., Cai, Z.W., Lu, Z.D., Zhang, X.L., & Wang, L. (2017), "Shear performance of bolted side-plated reinforced concrete beams", *Eng. Struct*., **144**(1), 73-87. https://doi.org/10.1016/j.engstruct.2017.04.043.

Li, X., Lv, H. and Zhou, S. (2012), "Flexural behavior of GFRP-reinforced concrete encased steel composite beams", *Constr. Build. Mater*., **28**(1), 255-262. https://doi.org/10.1016/j.conbuildmat.2011.08.058.

Liang, Q.Q., Uy, B., Bradford, M.A. and Ronagh, H.R. (2005), "Strength analysis of steel-concrete composite beams in combined bending and shear", *J. Struct. Eng*., **131**(10), 1593-1600. https://doi.org/10.1061/(ASCE)0733-9445(2005)131:10(1593).

Liu, D., Wang, F., Fu, F. and Wang, H. (2017), "Experimental research on the failure mechanism of foam concrete with C-Channel embedment", *Comput. Concrete*, **20**(3), 263-273. https://doi.org/10.12989/cac.2017.20.3.263.

Liu, M., Liang, M., Ma, Q., Wang, P. and Ma, C. (2020), "Web-post buckling of bolted castellated steel beam with octagonal web openings", *J. Constr. Steel Res.*, **164**, 1-15. https://doi.org/10.1016/j.jcsr.2019.105794.

Liu, T.C.H. and Chung, K.F. (2003), "Steel beams with large web opening of various shapes and sizes: finite element investigation", *J. Constr. Steel Res.*, **59**(9), 1159-1176. https://doi.org/10.1016/S0143-974X(03)00030-0.

Lubliner, J., Oliver, J., Oller, S. and Onate, E., (1989). "A plastic-damage model for concrete", *Int. J. Solid. Struct*., **25**(3), 299-326. https://doi.org/10.1016/0020-7683(89)90050-4.

Mahmoud, A.M. (2016), "Finite element modeling of steel concrete beam considering double composite action", *Ain Shams Eng. J.*, **7**(1), 73-88. https://doi.org/10.1016/j.asej.2015.03.012.

Mimoune, M., Soltani, M. and Bouchair, A. (2012), "Numerical modeling of castellated beams with hexagonal opening", *World J. Eng.*, **9**(2), 167-178. https://doi.org/10.1260/1708-5284.9.2.167.

Morkhade, S.G. and Gupta, L.M. (2015), "An experimental and parametric study on steel beams with web openings", *Int. J. Adv. Struct. Eng*., **7**, 249-260. https://doi.org/10.1007/s40091-015-0095-4

Moscoso, A.M., Tamayo, J.L. and Morsch, I.B. (2017), "Numerical simulation of external pre-stressed steel-concrete composite beams", *Comput. Concrete*, **2**(2), 191-201. https://doi.org/10.12989/cac.2017.19.2.191.

Nie, J., Tao, M., Cai, C.S. and Li, S. (2011), "Analytical and numerical modeling of prestressed continuous steel-concrete composite beams", *J. Struct. Eng*., **137**(12), 1405-1418. https://doi.org/10.1061/(ASCE)ST.1943-541X.0000409.

Qiao, P., Zou, G. and Davalos, J.F. (2003), "Flexural-torsional buckling of fiber-reinforced plastic composite cantilever I-beams", *Compos. Struct*., **60**(2), 205-217. https://doi.org/10.1016/S0263-8223(02)00304-5.

Redwood, R. and Demirdjian, S. (1998), "Castellated beam web buckling in shear", *J. Struct. Eng*., **124**(10), 1202-1207. https://doi.org/10.1061/(ASCE)07339445 (1998)124: 10(1202)

Salah, W. and Gizejowski, M.A. ((2008a), "Numerical finite element modeling of the stability behavior of slender section steel-concrete composite beams with web openings", *Proceedings Local Seminar of the polish Chapter of IASS*, Warsaw, 76-86.

Salah, W. and Gizejowski, M.A. (2008b), "Experimental investigation of the stability behavior of slender section steel-concrete composite beams with web openings", *Proceeding Local Seminar of the Polish Chapter of IASS*, Warsaw.

Sapountzakis, E.J. and Dourakopoulos, J.A. (2008), "Flexural-torsional buckling analysis of composite beams by BEM including shear deformation effect", *Mech. Res. Commun*., **35**(8), 497-516. https://doi.org/10.1016/j.mechrescom.2008.06.007.

Sener, K.C., Varma, A.H. and Seo, J. (2016), "Experimental and numerical investigation of the shear behavior of steel-plate composite (SC) beams without shear reinforcement", *Eng. Struct*., **127**(15), 495-509. https://doi.org/10.1016/j.engstruct.2016.08.053.

Shan, L. and Qiao, P. (2005), "Flexural-torsional buckling of fiber-reinforced plastic composite open channel beams", *Compos. Struct*., **68**(2), 211-224. https://doi.org/10.1016/j.compstruct.2004.03.015.

Sheehan, T., Dai, X., Lam, D., Aggelopoulos, E., Lawson, M. and Obiala, R. (2016), "Experimental study on long spanning composite cellular beam under flexure and shear", *J. Constr. Steel Res*., **116**, 40-54. https://doi.org/10.1016/j.jcsr.2015.08.047.

Vasdravellis, G. and Uy, B. (2014), "Shear strength and moment-shear interaction in steel-concrete composite beams", *J. Struct. Eng*., **140**(11), 04014084-040140811. https://doi.org/10.1061/(ASCE)ST.1943-541X.0001 008.

Vasudevan, G. and Kothandaraman, S. (2011), "Parametric study on nonlinear finite element analysis on flexural behaviour of RC beams using ANSYS", *Int. J. Civil Struct. Eng*., **2**(1), 98-111.

Vo, T.P. and Lee, J. (2007), "Flexural-torsional buckling of thin-walled composite box beams", *Thin Wall. Struct*., **45**, 790-798. https://doi.org/10.1016/j.tws.2007. 06. 001.

Vo, T.P. and Lee, J. (2007), "Flexural-torsional buckling of thin-walled composite box beams", *Thin Wall. Struct*., **45**, 790-798. https://doi.org/10.1016/j.tws.2007.06.001.

Warren, J. (2001), "Ultimate load and deflection behaviour of cellular beams", MSc Thesis, School of Civil Engineering, University of Natal, Durban, South Africa.

Weng, C.C., Yen, S.I. and Chen, C.C. (2001), "Shear strength of concrete-encased composite structural members", *J. Struct. Eng*., **127**(10), 1190-1997. https://doi.org/10.1061/(ASCE)0733-9445(2001)127:10(1190).

William, K.J. and Warnke, E.D. (1975), "Constitutive model for the triaxial behavior of concrete", *Proceeding of the International Assoc Bridge Structural Engineering*, Bergamo, 19-174.

Xu, C. and Wu, K (2019), "Damage and stiffness research on steel shape steel fibre reinforced concrete composite beams", *Comput. Concrete*, **24**(6), 513-525. https://doi.org/10.12989/cac.2019.24.6.513.

Yang, Y., Xue, Y., Yu, Y., Ma, N. and Shao, Y. (2017), "Experimental study on flexural performance of partially precast steel reinforced concrete beams", *J. Constr. Steel Res*., **133**, 192-201. https://doi.org/10.1016/j.jcsr.2017.02.019.

Zirakian, T. and Showkati, H. (2006), "Distortional buckling of castellated beams", *J. Constr. Steel Res.*, **62**(9), 863-871. https://doi.org/10.1016/j.jcsr.2006.01.004.

CC